Marta Serantes Melo

Study of the Stability of Encapsulated and Non-encapsulated Polymeric Photovoltaic Cells under Sun and Indoor illumination

MASTER'S DEGREE THESIS

supervised by Dr Josep Pallarès

MASTER'S DEGREE IN NANOSCIENCE, MATERIALS AND PROCESSES

UNIVERSITAT ROVIRA I VIRGILI

Tarragona

2022

Study of the Stability of Encapsulated and Non-encapsulated Polymeric Photovoltaic Cells under Sun and Indoor illumination

Marta Serantes Melo
Master Program in Nanoscience, Materials and Processes, 2021-2022
e-mail: marta.serantes@estudiants.urv.cat

Supervisor: Josep Pallarès.
Department of Electric, Electronic and Automatic Control. Universitat Rovira i Virgili
Campus Sescelades, c/. Marcel·lí Domingo, s/n Tarragona, 43007, Spain.

Abstract. In this study, we analyze the degradation behavior of conventional polymeric solar cells (PSCs) under both solar and indoor illumination. In addition, we compare the results obtained with encapsulated and non-encapsulated devices. The performance of the PTB7:$PC_{70}BM$-based cell showed an initial efficiency of 8.4 % under AM1.5G solar illumination and 12.0% under the LED one. The work describes first the results obtained after the measurement and analysis of the degradation process, performed by a current density – voltage (J–V) characteristic curve study, taking into account 4 performance parameters: power conversion efficiency (PCE), short circuit current density (J_{SC}), open-circuit voltage (V_{OC}) and fill factor (FF). The PCE of encapsulated devices under LED illumination decreased a 20% of the initial PCE after 624 h, while under sun illumination it lost a 90 % after 900 h. After this an impedance spectroscopy study was performed to analyze the internal evolution of the cell under solar AM1.5G illumination, getting to the conclusion that the active layer is the most affected when being encapsulated.

INTRODUCTION

Research in fields related to energy generation has been prominent for decades now because of fossil fuels, the main source nowadays, are scarce and have a negative impact on the environment, being one of the main causes of global warming and air pollution [1] [2]. The interest in finding clean and inexhaustible alternatives has led to the study of different natural resources, among which solar energy stands out, becoming a growing industry in both in commercial and home applications [1] [3]. However, there are many aspects that need to be investigated to achieve further development, which includes looking for organic materials capable of substituting silicon as the main active material in photovoltaic cells. One example are semiconducting organic polymers [1], which have advantages like being easier and cheaper to prepare, and are flexible and lightweight [4].

Active materials are the main component of solar cells, as they are the ones that react to light exposure causing the excitation of its electrons, and consequently transform the energy of light directly into electricity. This happens thanks to the movement of the through the semiconductor layers that form the device (Fig.1) [5]. The problem right now is that organic materials cannot display efficiencies comparable to silicon-based cells, and their degradation rates are unsatisfying. With everything, researchers have accomplished an increase in power conversion efficiency (PCE) from 6% to 17% (under AM 1.5G, 1000 W/m^2, solar radiation condition) thanks to the introduction of new materials, buffer layers and optimized fabrication conditions [6], which is really promising.

On a different note, something about organic cells that has attracted the attention of researches lately is their potential for indoor applications. In recent years the amount of electronic devices has increased exponentially, especially those related to communications that conform the Internet of Things (IoT) like wireless sensors and actuators [7]. This has motivated the investigation of ways to charge them without relying on batteries, in order to reduce their use and avoid inconveniences they cause to provide better reliability and operational lifetimes [8]. As a result, photovoltaic cells have become interesting for this purpose, seeing that electronic devices like IoT usually demand electrical power in ranges of 1 to 100 mW, something possible to achieve using cells that effectively react to artificial light. This has directed researchers to new areas of development that have not been widely studied yet [9].

The reason why organic solar cells are especially interesting for indoor applications is that organic materials have the ability to absorb radiance in the visible region of the light spectrum, ranging from 390 to 760 nm. This matches common artificial light used at offices and areas of very high visual demand, like LEDs [10], which require illuminations of at least 500 or 1000 lux [11].

Studies have proven to be really promising, reaching higher PCE than classic devices like crystal silicon solar cells [12], as the use of certain organic materials has led to PCE of over 23% under a 1000 lux LED [13].

Even after those positive results, the stability of the devices is still an unsatisfactory key aspect that stops their possibilities to be commercialized [14]. This is due to the active layer of organic cells being easily degraded by extrinsic and intrinsic factors like oxygen, water, heat, the diffusion of its materials, mechanical stress and photo-degradation [15]. As a result, encapsulation becomes an especially important process to achieve correct long-term performances by providing protection from external threats, and therefore a direct link to the stability of the device [16].

In addition, internal factors that affect degradation need to be also studied to understand the process that takes place at each one of the layers. Since interlayers also play an important role on the performance of the cell, it is interesting to perform progressive analysis under controlled environments to analyze photochemical reactions [17] [18]. It is the case of photo oxidation, which can happen at the different internal layers, but also at the metal electrodes [19]. In the case of polymer:fullerene cells, studies have concluded that the main degradation cause is UV irradiation because it alters both carrier mobility and the recombination process that creates current, leading to the decrease of PCE between other characteristic parameters [18] [20].

Studies have been commonly performed under sunlight but rarely under indoor light conditions, making it interesting to analyze if the same results occur in this spectral range.

To perform a complete degradation study several optoelectronic techniques need to be performed, including current density-voltage (J-V) and impedance spectroscopies. First, J-V measurements give basic information about PCE and parameters related to its resistance, which are necessary to characterize the behavior and potential of the cell. The impedance spectroscopy, in the other hand, gives information about the dielectric properties of the material. This properties can be later translated into an equivalent resistive/capacitive circuit model that describes the internal degradation of the cell layer by layer.

In this project, the degradation of conventional polymeric cells is performed using a copolymer called PTB7:$PC_{70}BM$ as the active layer. This material is composed by a semiconducting polymer (PTB7) and an ester, [6,6]-phenyl-C71-butyric acid methyl ester ($PC_{70}BM$).

The behavior of the cells is studied under both 1 sun illumination (standard reference AM 1.5G) and 1000 lux artificial LED 2700 K light over extended periods of time, following the Consensus stability testing protocols for organic photovoltaic materials and devices [21] to analyze whether they are interesting for indoor applications or not. The cells are kept under different controlled environments (nitrogen, air and also in air but encapsulated) to see how these elements affect their degradation too.

EXPERMENTAL SECTION

Fabrication and materials

The conventional structure chosen for this project was ITO/PEDOT:PSS/PTB7:$PC_{70}BM$/Ca/Ag. To start the fabrication of the 0.09 cm^2 organic cell, the pre-patterned glass substrates were carefully cleaned to remove any possible dust or residue. These substrates are coated with a first ITO layer that works as an anode. The deposition of the next layer, PEDOT:PSS that works as the electron blocking layer (EBL) was achieved by spin coating it at 4000 rpm for 40 s. After that, the samples were put in a heating plate for 15 min at 150ºC for thermal annealing. The rest of the process was performed inside a glove box under inert nitrogen environment to guarantee no impurities interfere in the process. The active layer solution has to be prepared in advance, mixing the PTB7 and $PC_{70}BM$ (1:1.5 weight ratio) in chlorobenzene and 1,8-diiodooctane (97:3 by volume) to get a 25 mg L^{-1} concentration. The solution needs to age for 48 hours before spin coating it for 30s at 750 rpm to get a 100 nm width layer. The last two layers, a hole blocking layer (HBL) and a cathode conformed by 25 nm of Ca and 100 nm of Ag respectively, were added by applying a thermal evaporation procedure inside a vacuum chamber under high pressure conditions. Some of the samples were later encapsulated using an UV-curing liquid acrylic adhesive, using copper to restore the contacts.

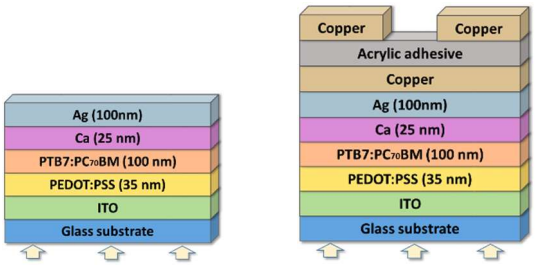

Figure 1. *Structure of non-encapsulated and encapsulated devices.*

Studied solar cells

Table 1. *Description of the studied solar cells.*

Sample	Illumination	Environment	Encapsulation
L13	Sun	Nitrogen	No
Q14	Sun	Air	Yes
Q6	Indoor	Air	Yes
Q12	Indoor	Air	No

Measurements

To perform the analysis two main techniques were applied:

- Current density-voltage (J-V)

Study both under simulated solar illumination (equivalent to 1 sun) using an Abet Technologies model Sun 2000 (Milford, CT) simulator and 1000 lux artificial LED 2700 K bulb. A Keithley 2400 (Cleveland, OH) measurement unit is used for the recollection of the data. The program used for the visualization of the results is Origin 9.0.

- Impedance spectroscopy (IS)

Same illumination conditions, but using a HP-4192A impedance analyzer. The study is performed applying a 0.05 oscillation level and a voltage of 0.8 V as spot bias. The frequency step used is 1000 Hz, and the main start and stop values 100 and 5 MHz respectively. These values might change in some measures depending on the results to achieve better fitting ones. After that, the results are fitted to equivalent electrical models.

RESULTS AND DISCUSSION

J-V

Sun study

Figure 2 shows the curves obtained through a J-V analysis of encapsulated and non-encapsulated devices under sun-simulated lighting (AM1.5G). It can be appreciated that curves from the encapsulated one (Q14) progressively change notably over time, just like in the non-encapsulated ones (L13). This means both have gone through a degradation process, as curves lose amplitude.

Electrical parameters displayed at the normalized graphs (***Figure 3***) show how in encapsulated cell they decreased over time, with open-circuit voltage (V_{OC}) staying mainly stable during the first 700 h before going down in a 30 % of its initial value. Short-circuit current density (J_{SC}), fill factor (FF) and the efficiency decreased notably more, getting down in a 65 %, 70 % and 90 % after 1000 h. Efficiency started at 5.54 % and ended at 0.44 %.

In the case of L13 (non-encapsulated and stored in nitrogen), it maintained its values much stable with V_{OC} only decreasing in a 5 % and J_{SC} in a 10 %, while FF and efficiency went down in a 30 % and 45 % respectively in a similar tendency. There is a drastic and non-expected change at the last two points, probably due to damaging of the contacts during the manipulation of the cell. Note that this cell was stored under an inert environment and not ambient conditions, which definitely helped maintain its characteristics longer for the lack of external factors like water and oxygen.

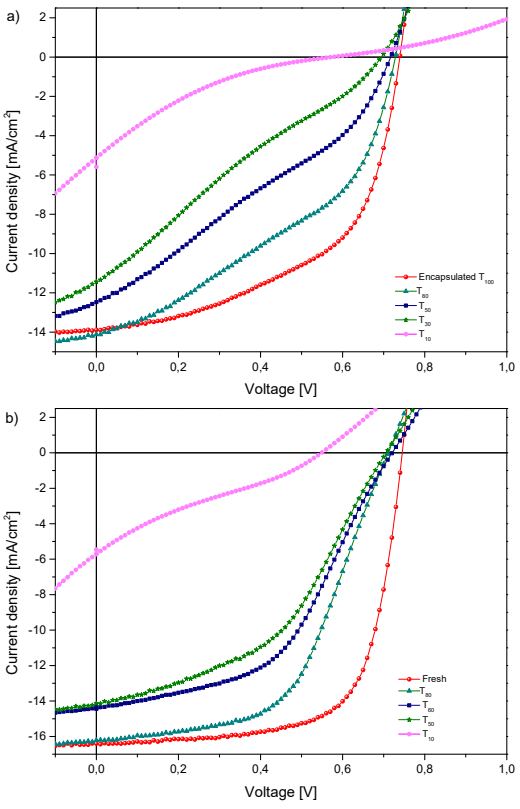

Figure 2. *J-V characteristics of a) encapsulated (Q14) and b) non-encapsulated (L13) cells under AM1.5G illumination. Progression after certain level of degradation (T_{80} = 80 % of the initial value).*

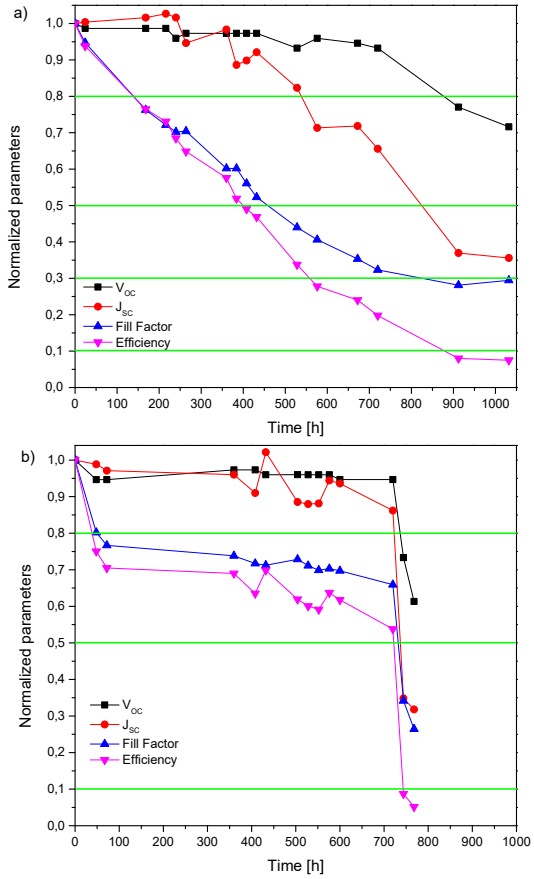

Figure 3. *Normalized parameters obtained through J-V analysis of a) encapsulated (Q14) and b) non-encapsulated (L13) solar cells.*

Figure 4 represents an example of the characteristics obtained applying the same J-V study under dark illumination. This gives more information about the performance of the devices when there is a low level of illumination.

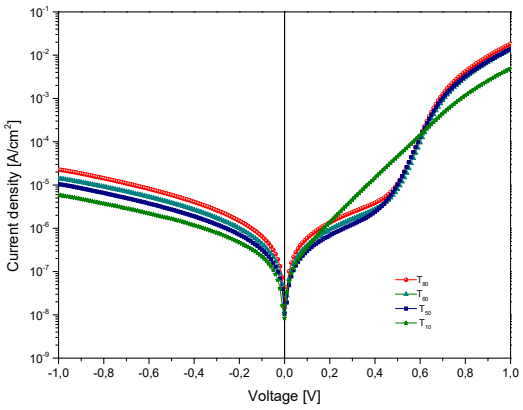

Figure 4. *J-V characteristics of the non-encapsulated (L13) solar cell under dark illumination.*

The main thing that can be observed is how the positive part of the graph decreases with time, which means series resistance (R_S) is getting lower. This can be confirmed by representing the progression of the resistances over time, as in ***Figure 5***. This figure represents both R_S and parallel resistance (R_{SH}).

There is a similar tendency in the parameters of both encapsulated and non-encapsulated cell, with R_S increasing while R_{SH} goes down.

In the non-encapsulated cell there is a fast reduction in R_{SH} during the first 50 h, getting from 2153 to 570 Ω cm^2, and then oscillating around 300 Ω cm^2. In the other hand, in the encapsulated one the initial value was lower, at 510 Ω cm^2 and quickly decreased to 193 Ω cm^2 in the next 168 h, finally ending at 58 Ω cm^2.

However, R_S started al low values in both samples, about 3 Ω cm^2, and slowly went up to about 17 Ω cm^2 in the case of the non-encapsulated one. The encapsulated cell stayed mainly stable until reaching 700 h, when it got to 50, and then ended at 227.5 Ω cm^2 after another 212 h.

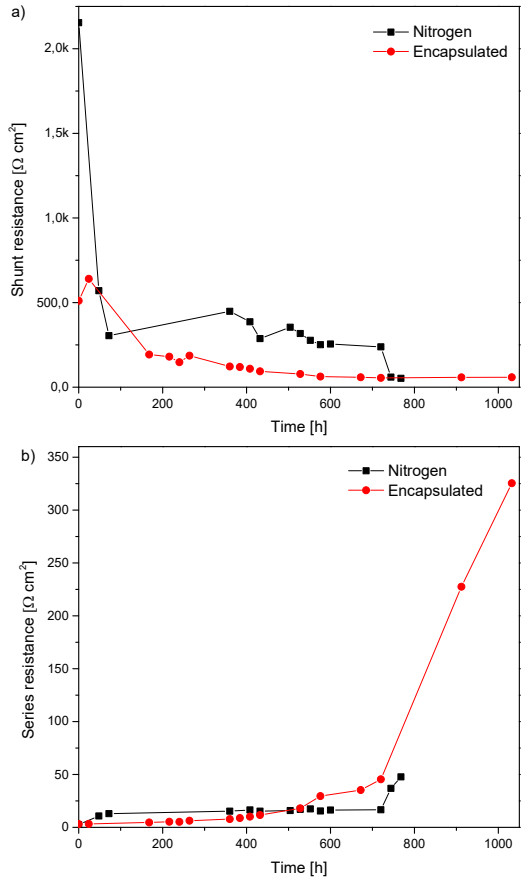

Figure 5. *Evolution of a) series resistance and b) parallel resistance over time in encapsulated (Q14) and non-encapsulated cells stored in nitrogen (L13).*

Figure 6 shows the representation of solar cells under both dark and light illumination. This graph represents different characteristics, with V_{OC} appearing as the lower peak at the light illumination line, and J_{SC} at the point it crosses 0 V. The area between both lines corresponds to

the Energy generated by the cell, as it shows the difference between the moment in which there is incident light and when there is not. In addition, comparing both graphs it is possible to see how the line that corresponds to the illuminated cell decreases slightly at the starting point because of degradation.

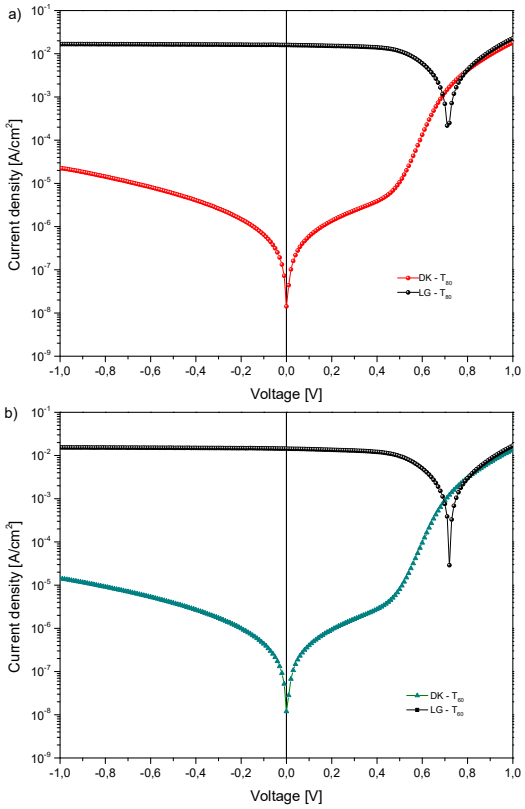

Figure 6. *J-V characteristics of non-encapsulated solar cells (L13) under dark (DK) and light (LG) illumination at levels of degradation of a) T80 and b) T60.*

Indoor study

Figure 7 display the characteristics obtained through a J-V analysis of encapsulated and non-encapsulated devices under indoor LED illumination. At first sight is possible to see that the curves from the encapsulated one (Q6, ***Figure 7***a) barely change with time, which means the cell is pretty stable. In the other hand, the curves of non-encapsulated cell move progressively to the left, losing amplitude due to continuous degradation.

In the case of the encapsulated sample V_{OC} and J_{SC} stay practically the same with barely a 5 % of loss. However, the efficiency follows a similar tendency to the FF decreasing almost a 30 % from their initial values. This way, the initial power conversion efficiency was 12.02 % and got to 8.56 % after 936 hours.

In contrast, the non-encapsulated cell shows a clear reduction in the four parameters displayed at the normalized graph (***Figure 8***). In this one V_{OC} and FF are affected in a similar way, ending with almost a 40 % reduction and with J_{SC} reaching a 30 %. The efficiency sees itself affected by all those factors, decreasing to close to the 25 % of the initial value. The most drastic change is seen during the first 100 hours in which efficiency goes down in a 55 %. This fast and abrupt decrease is known as "burn-in loss", and is one of the main causes of the short lifetime of polymer solar cells [22].

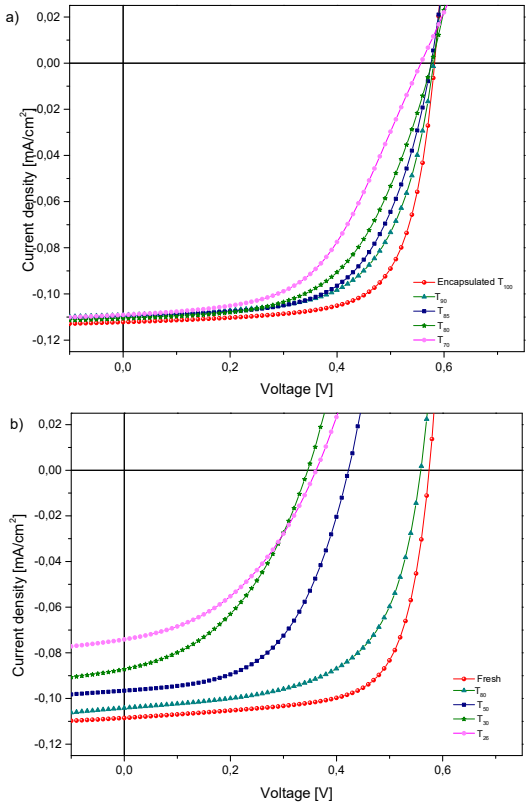

Figure 7. *J-V characteristics of a) encapsulated (Q6) and b) non-encapsulated (Q12) cells under indoor illumination. Progression after certain level of degradation (T80 = 80 % of the initial value).*

About the images that represent resistance (***Figure 9***) both in R_S and R_{SH}, we can appreciate similar tendencies in the change of encapsulated and non-encapsulated devices, with R_S increasing while R_{SH} is reduced. In the case of the non-encapsulated cell there is a fast increase during the first 360 h in R_S, reaching 403 Ω cm^2, and then stabilizing in parameters between 250 and 300 Ω cm^2. However, in the encapsulated one the increase was visibly smaller, going from 5 to 100 Ω cm^2 after the same time, even though it sped up again after 672 h.

The results obtained about both resistances correspond with the observed progression of the degradations. Firstly, increases in R_S especially affect the

fill factor and efficiency, which explains their fast decrease in the non-encapsulated cell during the first hours while R_S steps up in a quick way. This happens because series resistance is caused by the movement of current between both contacts, and also the resistance between them [23].

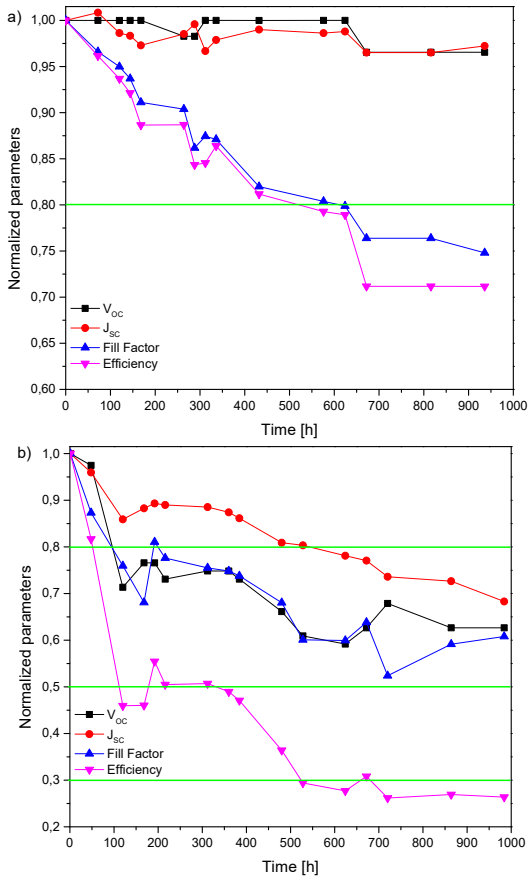

Figure 8. *Normalized parameters obtained through J-V analysis of a) encapsulated (Q6) and b) non-encapsulated (Q12) solar cells.*

However, J_{SC} might be reduced if R_S becomes extremely high, and the reason why V_{OC} is not affected by this resistance is that current flows directly through the device near the open-circuit voltage [24]. In addition, decreases in R_{SH} lead to losses because of power reduction [23]. This happens because R_{SH} provides an alternate path for light-generated current, affecting the recombination of charge carriers. This way the amount of current that flows through is reduced, and therefore, the voltage of the cell [25].

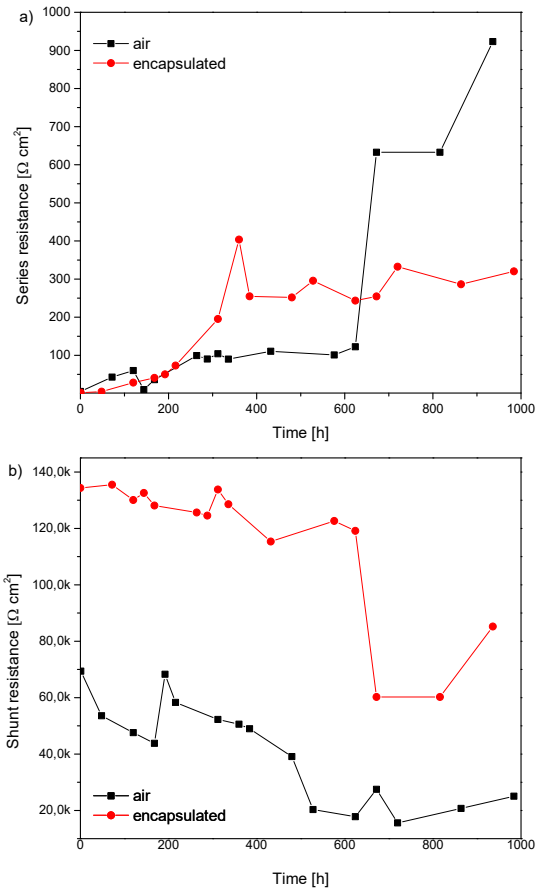

Figure 9. *Evolution of a) series resistance and b) parallel resistance over time in encapsulated and non-encapsulated cells.*

All of these values confirm the positive consequences of applying an encapsulation to the devices, as it protects them from extrinsic factors like oxygen, and water [15]. In addition, non-encapsulated cells are faster degraded because of being affected by both extrinsic and intrinsic factors which easily degrade the active layer in organic cells. Research have concluded that one of their possible main degradation causes is UV irradiation because it alters both carrier mobility and the recombination process that creates current, leading to the decrease of PCE between other characteristic parameters [21].

What is more, R_S and R_{SH} are generally correlated with the physical properties of the active layer and the architecture of the device. Therefore, it would be interesting to choose the structure and materials capable of reducing the value of R_S and maximizing R_{SH} [23].

More quantitative information about the different parameters can be found at the tables present at the Annex (Supplementary Information, ***Table 2*** and ***Table 3***).

Impedance spectroscopy

In this part of the study an impedance spectroscopy is performed to analyze which one of the layers is more degraded over time. To achieve this, the results are fitted to equivalent electrical models. These circuits are formed by three elements (resistors or capacitors) placed in series, in which each element will be associated to a certain layer of the cell, allowing their analysis independently.

Each layer will be equivalent to a capacitor and resistance placed in parallel as displayed in ***Figure 10*** [26].

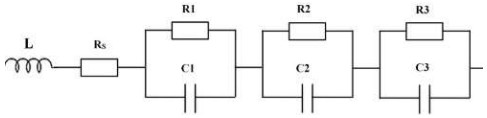

Figure 10. *Equivalent 3RD circuit.*

In this case R1C1 corresponds to the PEDOT:PSS layer, R2C2 to PTB7:$PC_{70}BM$ and lastly R3C3 to Ca.

To perform the analysis is necessary to know the capacitance of each layer based on the material it is formed by, using the formula at ***Equation 1,*** where C is the capacitance (F), ε_0 is the vacuum permittivity (F/m), $\varepsilon_{layer}$is the permittivity of the material (F/m), A the area of the device and d_{layer} the thickness of the layer (m).

$$C = \varepsilon_0 \varepsilon_{layer} \frac{A}{d_{layer}}$$

Equation 1: Capacitance formula.

The measurements were performed using a HP-4192A impedance analyzer, applying a 0.05 oscillation level and a voltage of 0.8 V as spot bias. The frequency step used is 1000 Hz, and the main start and stop values 100 and 5E+6 Hz respectively.

Figure 11 shows the Cole-Cole plots obtained through this method for two cells under AM1.5G solar illumination, one non-encapsulated (L13) and the other encapsulated (Q14). Firstly, it can be noticed that all of them form semicircles, which is the typical shape of circuits conformed by RC elements. In addition, the radius of those arcs increases with time, as it is expected because of the degradation of the devices. In this case the non-encapsulated cell reached higher values, even though it was the encapsulated one that increased at a higher rate, multiplying by 5 its initial value.

It can also be observed that some of the arcs do not close on the X axis, as they cannot reach an impedance of zero at such high frequencies.

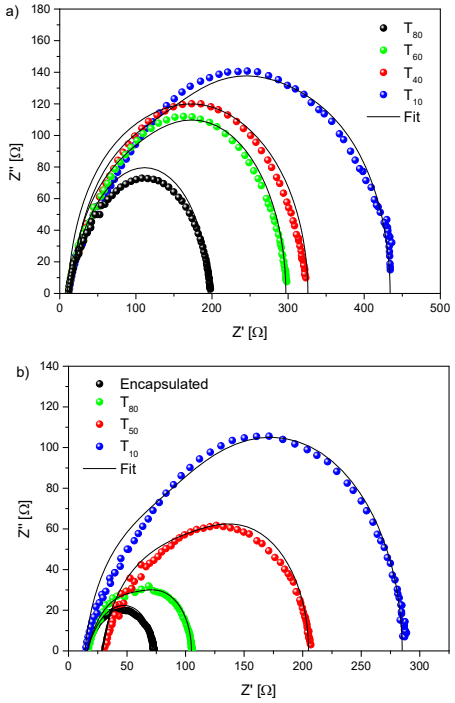

Figure 11. *Cole–Cole plots of the a) non-encapsulated (L13) and b) encapsulated (Q14) solar cells under AM1.5G illumination.*

Once impedance results have been modelled, values of capacitance and resistance of each layer over time are extracted. These are displayed in ***Figure 12*** and ***Figure 13***.

Firstly, theoric capacitances are calculated using the formula in ***Equation 1.***

These work as the initial values, with C1 = 5.01 nF, C2 = 3.11 nF and C3 = 9.56 nF. The different values used for the calculus are displayed at the Data annex (***Table 4***). Analyzing then the results obtained over time, in the case of the non-encapsulated cell stored in nitrogen (***Figure 12*** a) the capacitance of the calcium layer (C3) increased notably while the other two stayed mostly stable while. On the other hand, in the encapsulated one (***Figure 12*** b) the PEDOT:PSS layer (C1) increased in almost the same amount as calcium. The active layer (C2) stays mostly the same in both, being the lower value of the three layers.

At first it could be expected to have less changes in the encapsulated cell, but it has to be considered that it is stored in air while the other is under an inert environment. This means the PEDOT:PSS layer was probably affected by extrinsic factors like air or humidity, that are still more present in the encapsulated. However, calcium did increase less when encapsulated.

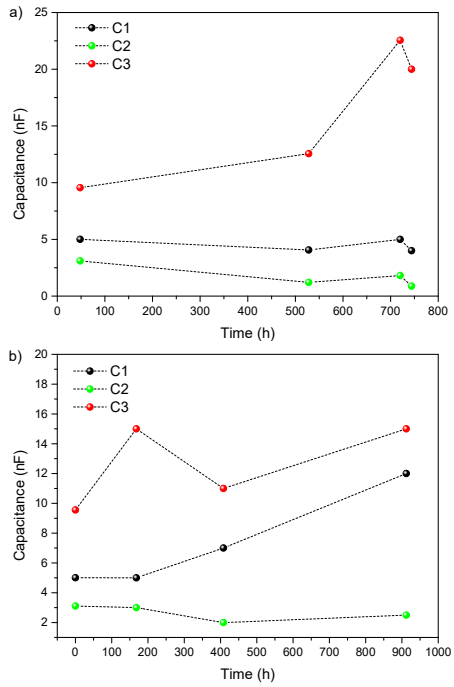

Figure 12. *Capacitances of a) non-encapsulated (L13) and b) encapsulated (Q14) solar cells over time under AM1.5G illumination. C1 (black) correspond to the PEDOT:PSS layer, C2 to PTB7:PC$_{70}$BM (green) and lastly C3 to calcium (red).*

About the resistances, the results of the non-encapsulated cell (***Figure 13*** **a)** show a moderate increase, with PTB7:PC$_{70}$BM (R2) being the most affected (about 80 Ω) and calcium the least (about 65 Ω) after 400 h. There is a more prominent increase in all the layers after 700 h, but as commented in the efficiency it can be a consequence of damage during the manipulation of the cell. In the case of the encapsulated one (***Figure 13*** **b**), the PEDOT:PSS and calcium layers increase in a similar manner in about 55 Ω. However, the active one (R2) goes up in almost 100 Ω, being the most affected.

Seeing the results, in the encapsulated cell it is the active layer which is the most affected. This is probably due to the material being the most sensible one to photo degradation, in addition to the possible consequences from the contact with other external factors. This explains why it has been more affected than in the non-encapsulated one, as even though it is more physically protected it is stored in air, while the non-encapsulated was preserved under an inert environment. Calcium is also affected but in smaller amounts, and PEDOT:PSS displays similar evolution in both cases.

This means keeping the cells under controlled nitrogen conditions achieves better results than encapsulation in relation to the active layer.

More quantitative information about the parameters can be found at the tables present at the Annex (Supplementary Information, ***Table 5***).

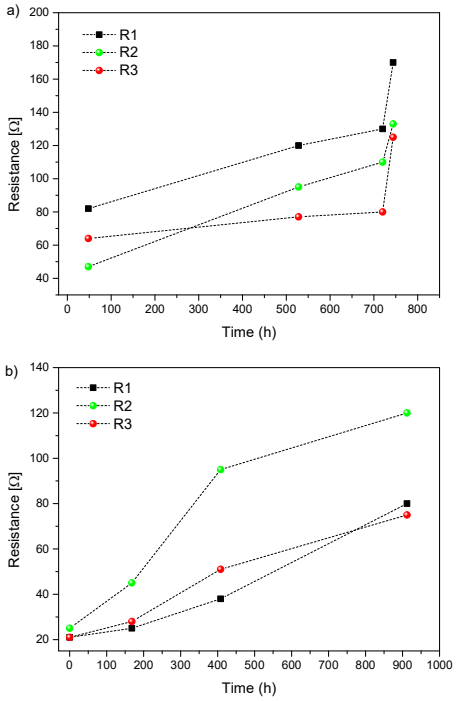

Figure 13. *Resistances of a) non-encapsulated (L13) and b) encapsulated (Q14) solar cells over time under AM1.5G illumination. R1 (black) correspond to the PEDOT:PSS layer, R2 to PTB7:PC$_{70}$BM (green) and lastly R3 to calcium (red).*

CONCLUSIONS

A first analysis on the degradation of conventional polymer:fullerene organic solar cells, based on PTB7:PC$_{70}$BM as their active layer, can be performed thanks to the study of J-V and impedance characteristics.

In a general manner, it can be observed that there is a progressive degradation due to J-V curves becoming visually smaller and less steep. In addition, the normalized parameters show a fast decrease during the first hours called “burn-in-loss” in several samples.

Comparing results it can be observed that storing the cells under a nitrogen environment (L13) helps maintain the different parameters quite stable, not getting below a 50 % in any of them after 700 h when measured under solar illumination. In the other hand, when encapsulated and stored in air, the final values become much lower, with efficiency ending at barely 20 % of the initial one after the same time.

The results were different when studied under LED light, as in the encapsulated cell the efficiency only decreased in a 30 %, and V_{OC} and J_{SC} stayed almost constant. In the non-encapsulated, however, efficiency decreased to almost the 15 %, confirming the effect of environmental factors on the cell.

The difference between the encapsulated cells under solar and LED illumination implies that sunlight damages more the active layer in organic cells than the indoor do.

About the Impedance Spectroscopy analysis, the study allowed to know which one of the layers was more affected by degradation thanks to its fitting to an RC equivalent circuit model, giving information about what happens inside the device. This correlation, in which each layer corresponds to an RC element, also explains the evolution of both, resistance and capacitance of each layer over time. The study led to the conclusion that the active layer is the most affected one when the cell is encapsulated, probably due to photo degradation. For cells stored in nitrogen both the active layer and the PEDOT:PSS contribute to the loss of cell performance.

ACKNOWLEDGES

This work was supported by Ministerio de Ciencia e Innovación under Grant PDI2021-128342OB-I00; Diputació de Tarragona under Grant 2021CM14 and 2022PGR-DIPTA-URV04; the Spanish Ministry of Science and Innovation (MICINN/FEDER) under Grant RTI2018-094040-B-I00; the Agency for Management of University and Research Grants (AGAUR) under ref. 2017-SGR-1527. In addition, its performance was carried out under the supervision of the Nephos group, from the Department of Electric, Electronic and Automatic Control at the Universitat Rovira I Virgili, situated in Tarragona, Spain. I also want to thank Magaly Ramírez-Como for her help through all the experimental and analytic part of the process.

REFERENCES

[1] S. Ananthakumar, J. R. Kumar and S. M. Babu, "Third-Generation Solar Cells: Concept, Materials and Performance - An Overview," in *Emerging Nanostructured Materials for Energy and Environmental Science. Environmental Chemistry for a Sustainable World vol. 23*, vol. 23, Springer, Cham, 2019, pp. 205-339.

[2] F. Martins, C. Felgueiras, M. Smitkova and N. Caetano, "Analysis of Fossil Fuel Energy Consumption and Environmental Impacts in European Countries," *Energies,* vol. 12(6), no. 964, 2019.

[3] Y. Chu and P. Meisen, "Review and Comparison of Different Solar Energy Technologies," Global Energy Network Institute, 2011.

[4] P. Chengac and X. Zhan, "Stability of organic solar cells: challenges and strategies," *Chem. Soc. Rev.,* vol. 45, no. 2544, pp. 2544--2582, 2016.

[5] P. Ciambelli, G. La Guardia and L. Vitale, "Chapter 7 - Nanotechnology for green materials and processes," in *Studies in Surface Science and Catalysis*, vol. 179, Italy, 2020, pp. 97-116.

[6] A. Gusain, R. M. Faria and P. B. Miranda, "Polymer Solar Cells—Interfacial Processes Related to Performance Issues," *Front. Chem.,* vol. 7, no. 51, pp. 1-25, 2019.

[7] J. Gubbi, R. Buyya, S. Marusic and M. Palaniswami, "Internet of Things (IoT): A vision, architectural elements, and future directions," *Future Generation Computer Systems,* vol. 29, no. 7, pp. 1645-1660, 2013.

[8] I. Mathews, S. N. Kantareddy and I. M. Peters, "Technology and Market Perspective for Indoor Photovoltaic Cells," *Joule,* vol. 3, pp. 1415-1426, 2019.

[9] L.-K. Ma, Y. Chen, P. C. Chow, K. S. Wong, S. K. So and H. Yan, "High-Efficiency Indoor Organic Photovoltaics with a Band-Aligned Interlayer," *Joule,* vol. 4, pp. 1486-1500, 2020.

[10] C. L. Cutting, M. Bag and D. Venkataraman, "Indoor light recycling: a new home for organic photovoltaics," *Journal of Materials Chemistry,* vol. 4, pp. 10367-10370, 2016.

[11] I. N. d. S. e. H. e. e. Trabajo, "Real Decreto 486/1997, de 14 de abril. Guía Técnica para la Evaluación y Prevención de los Riesgos Relativos a la Utilización de los Lugares de Trabajo".

[12] S. Mori, T. Gotanda, Y. Nakano, M. Saito, K. Todori and M. Hosoya, "Investigation of the organic solar cell characteristics for indoor LED light applications," *Japanese Journal of Applied Physics,* vol. 54, no. 7, 2015.

[13] Y.-J. You, C. E. Song, Q. V. Hoang, Y. Kang, J. S. Goo, D.-H. Ko, J.-J. Lee, W. S. Shin and J. W. Shim, "Highly Efficient Indoor Organic Photovoltaics with Spectrally Matched Fluorinated Phenylene-Alkoxybenzothiadiazole-Based Wide Bandgap Polymers," *Advances Functional Materials,* vol. 29, no. 27, 2019.

[14] W. Chen, J. Zhang, G. Xu, R. Xue, Y. Li, Y. Zhou, J. Hou and Y. Li, "A Semitransparent Inorganic Perovskite Film for Overcoming Ultraviolet Light Instability of Organic Solar Cells and Achieving 14.03% Efficiency," *Advanced*

Materials, vol. 30, no. 1800855, 2018.

[15] L. Duan and A. Uddin, "Progress in Stability of Organic Solar Cells," *Advanced Science,* vol. 7, no. 11, 2020.

[16] K. Aitola, G. G. Sonai, M. Markkanen, J. J. Kaschuk, X. Hou, K. Miettunen and P. D. Lund, "Encapsulation of commercial and emerging solar cells with focus on perovskite solar cells," *Solar Energy,* vol. 237, pp. 264-283, 2022.

[17] S. Park and H. J. Son, "Intrinsic photo-degradation and mechanism of polymer solar cells: the crucial role of non-fullerene acceptors," *Journal of Materials Chemistry A,* vol. 7, no. 45, p. 25675–26188, 2019.

[18] A. Sharma, M. Chauhan, J. Patel, M. K. Pandey, . B. Tripathi, . J. P. Tiwari and S. Chand, "Study of light-induced degradation of polymer: fullerene solar cells," *New Journal of Chemistry,* 2022.

[19] E. Osorio, J. G. Sánchez, L. N. Acquaroli, M. Pacio, J. Ferre-Borrull, J. Pallarès and L. F. Marsal, "Degradation Analysis of Encapsulated and Nonencapsulated TiO2/PTB7:PC70BM/V2O5 Solar Cells under Ambient Conditions via Impedance Spectroscopy," *ACS Omega,* vol. 2, p. 3091−3097, 2017.

[20] P. B. R. M.-O. A. E. X. M. M. R. B. A. B. V. R. M. J. Romero, "Enhanced stability in semi-transparent PTB7/PC71BM photovoltaic cells.," *Solar energy materials and solar cells,* vol. 137, pp. 44-49, 2015.

[21] M. Reese, S. Gevorgyan, M. Jørgensen, E. Bundgaard, S. Kurtz, D. Ginley, D. Olson, M. Lloyd, P. E. Katz, A. Elschner, O. Haillant, T. Currier, V. Shrotriya, M. Hermenau, M. Riede, K. Kirov, G. Trimmel and F. Krebs, "Consensus stability testing protocols for organic photovoltaic materials and devices," *Solar Energy Materials & Solar Cells,* vol. 95, no. 5, pp. 1253-1267, 2011.

[22] J. Kong, S. Song, M. Yoo, G. Young Lee, O. Kwon, J. K. Park, H. Back, G. Kim, S. H. Lee, H. Suh and K. Lee, "Long-term stable polymer solar cells with significantly reduced burn-in loss," *NATURE COMMUNICATIONS,* vol. 5, no. 5688, 2014.

[23] F. F. Muhammadsharif, Y. Y. Mohd, S. S. Hameed, F. Aziz, K. Sulaiman, M. A. Rasheed and Z. Ahmad, "Employment of single-diode model to elucidate the variations in photovoltaic parameters under different electrical and thermal conditions," *PLOS ONE,* vol. 12, no. 8, 2017.

[24] C. Honsberg and S. Bowden, "PVCDROM," [Online]. Available: https://www.pveducation.org/pvcdrom/solar-cell-operation/series-resistance.

[25] C. Honsberg and S. Bowden, "PVCDROM," [Online]. Available: https://www.pveducation.org/pvcdrom/solar-cell-operation/shunt-resistance.

[26] A. K. Jonscher, "Dielectric relaxation in solids," *Journal of Physics D: Applied Physics,* vol. 32, no. 14, 1999.

Annex: Supplementary Information

Data annex

Table 2. *Current density – voltage characteristics of solar cells studied under light illumination.*

Sample	Degradation (%)	Time (h)	V_{OC} (V)	J_{SC} (mA/cm^2)	FF	PCE (%)	R_S (Ω cm^2)	R_{SH} (kΩcm^2)
Q6	Fresh	0	0.58	0.112	0.70	12.03	5.00	134.34
	T90 (~88.66)	168	0.58	0.109	0.64	10.66	36.12	128.11
	T85 (~86.40)	336	0.58	0.110	0.61	10.39	90.10	128.57
	T80 (~79.28)	576	0.58	0.111	0.56	9.54	100.77	122.66
	T70 (~71.16)	936	0.56	0.109	0.53	8.56	923.28	85.20
Q12	Fresh	0	0.57	0.109	0.69	11.37	1.92	69.39
	T80 (~81.68)	48	0.56	0.104	0.61	9.29	4.63	53.57
	T50 (~50.49)	216	0.42	0.097	0.54	5.74	73.11	58.31
	T30 (~29.41)	528	0.35	0.087	0.42	3.34	295.65	20.33
	T25 (~26.36)	984	0.36	0.074	0.42	3.00	320.31	25.06
L13	Fresh	0	0.75	16.4	0.68	8.42	2.61	2153.60
	T80 (~75.04)	48	0.71	16.21	0.55	6.32	10.73	570.15
	T60 (~60.06)	528	0.72	14.43	0.49	5.06	17.01	317.25
	T50 (~53.79)	720	0.71	14.13	0.45	4.53	16.61	238.38
	T10 (~8.72)	744	0.55	5.71	0.23	0.73	36.85	59.41
Q14	Fresh	0	0.74	13.89	0.54	5.54	3.08	510.62
	T80 (~76.47)	168	0.73	14.11	0.41	4.24	4.65	193.05
	T50 (~49.02)	408	0.72	12.48	0.30	2.72	10.12	109.16
	T30 (~33.77)	528	0.69	11.44	0.24	1.87	18.02	78.00
	T10 (~8.00)	912	0.57	5.13	0.15	0.44	227.49	58.07

Table 3. *Current density – voltage characteristics of solar cells studied under dark conditions.*

Sample	Degradation (%)	Time (h)	Voltage (V)	Current (A)	R Series (Ω cm^2)	R Parallel (kΩcm^2)
Q6	Fresh	0	1.21E-05	-6.17E-10	17.36	11996.44
	T90 (~88.66)	168	1.47E-05	-1.44E-10	21.77	13085.92
	T85 (~86.40)	336	1.37E-05	1.98E-09	653.73	1174.50
	T80 (~79.28)	576	1.63E-05	2.21E-10	376.85	15952.80
	T70 (~71.16)	936	1.41E-05	5.08E-10	3184.58	10466.60
Q12	Fresh	0	1.25E-05	5.48E-10	15.37	6303.18
	T80 (~81.68)	48	1.21E-05	3.33E-10	17.99	4765.77
	T50 (~50.49)	216	1.25E-05	2.26E-09	188.53	560.97
	T30 (~29.41)	528	1.46E-05	7.74E-10	544.20	243.56
	T25 (~26.36)	984	1.56E-05	5.05E-09	728.78	476.85
L13	T80 (~75.04)	48	1.35E-05	-1.28E-09	88.35	167.24
	T60 (~60.06)	528	1.06E-05	-1.08E-09	119.24	246.13
	T50 (~53.79)	720	1.45E-05	-9.43E-10	115.33	335.34
	T10 (~8.72)	744	1.63E-05	7.57E-10	322.65	377.31
Q14	T80 (~76.47)	168	1.55E-05	3.61E-10	36.33	26260.87
	T50 (~49.02)	408	1.67E-05	3.50E-10	76.93	22020.33
	T30 (~33.77)	528	1.60E-05	1.88E-09	99.92	1.27
	T10 (~08.00)	912	1.65E-05	1.40E-09	2260.28	39.83

Table 4. *Values used for the calculus of each layer's capacitance.*

Layer	ε_0 (F/m)	Area (m^2)	ε_{layer} (F/m)	Thickness (m)	Capacitance (F)	Capacitance (nF)
PEDOT:PSS	8,85E-12	0,000009	2.2	3.5E-8	5.01E-9	5.01
PTB7:$PC_{70}BM$	8,85E-12	0,000009	3.9	1.0E-7	3.11E-9	3.11
Ca	8,85E-12	0,000009	3	2.5E-8	9.56E-9	9.56

Table 5. *Capacitance and resistance values of the different layers obtained through impedance spectroscopy.*

Sample	Degradation (%)	Max. Z'' (Ω)	C1 (nF)	C2 (nF)	C3 (nF)	R1 (Ω)	R2 (Ω)	R3 (Ω)
L13	T80	73	5.01E-9	3.11E-9	9.56E-9	82	47	64
	T60	112	4.07E-9	1.21E-9	1.26E-8	120	95	77
	T50	120	5.00E-9	1.81E-9	2.26E-8	130	110	80
	T10	141	4.00E-9	8.80E-10	2.00E-8	170	133	125
Q14	encapsulated	20	5.01E-9	3.11E-9	9.56E-9	21	21	25
	T80	32	5.00E-9	3.00E-9	1.5E-8	25	28	45
	T50	62	7.00E-9	2.00E-9	1.1E-8	38	51	95
	T10	106	1.20E-8	2.50E-9	1.5E-8	80	75	120

Images annex

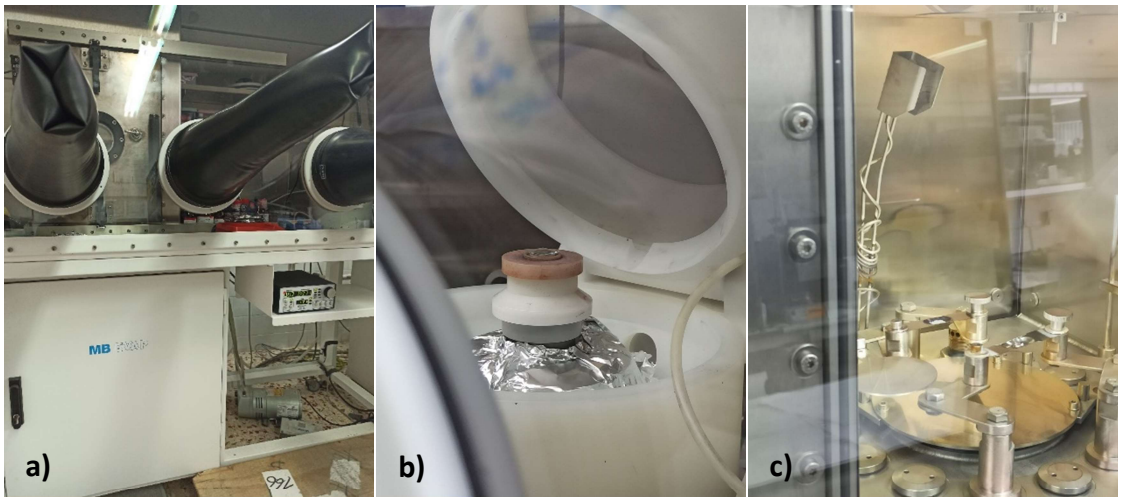

Figure 14. *Fabrication equipment: a) glove box, b) thermal evaporation chamber and c) spinner.*

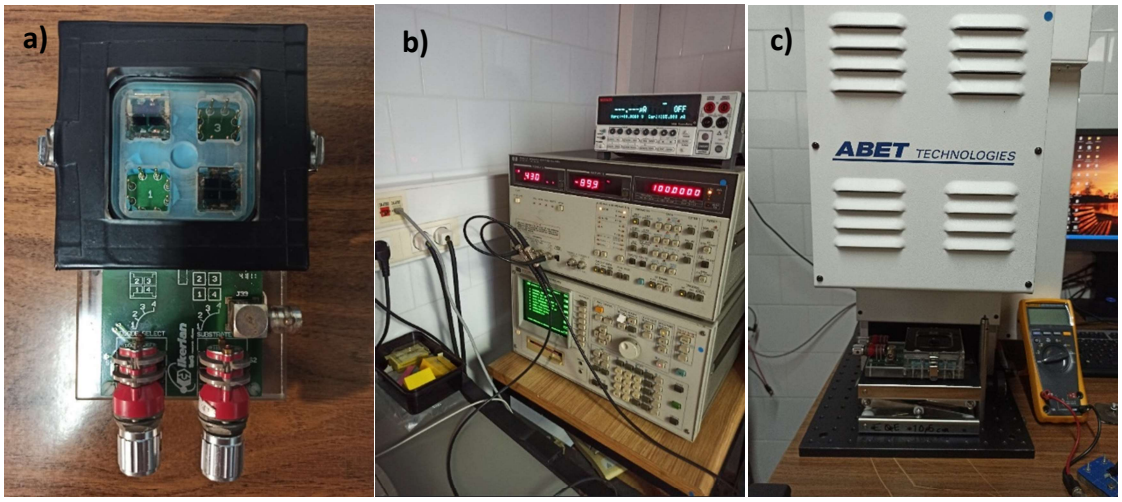

Figure 15. *Measurement equipment: a) solar cell holder, b) measurement unit (Keithley 2400. Cleveland, OH) and impedance analyzer (HP-4192A) and c) solar simulator (Abet Technologies model Sun 2000. Milford, CT).*

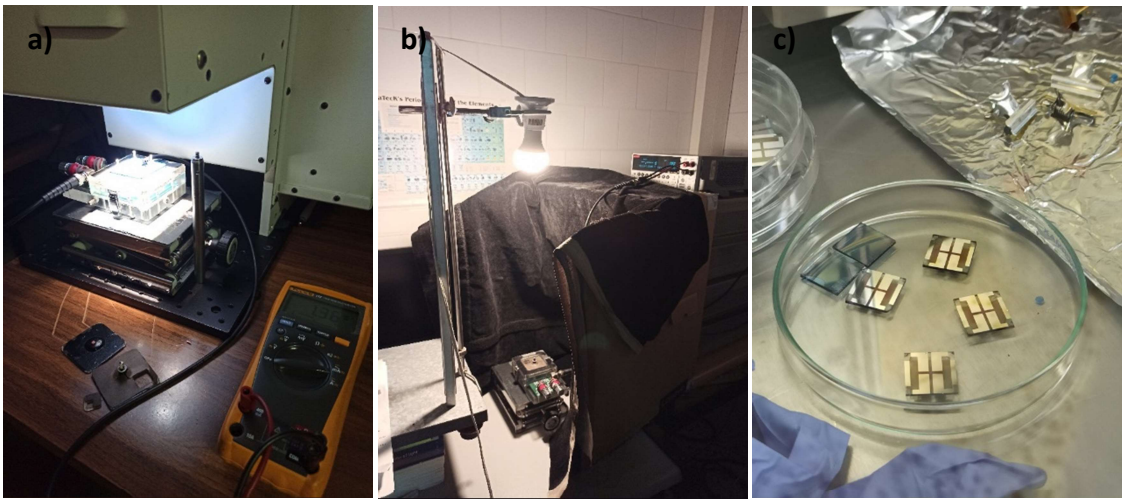

Figure 16. *Final assembly a) solar illumination, b) 1000 lux artificial LED 2700 K light and c) fabricated solar cells.*